

1 **SUPPORTING INFORMATION**

2  
3 **TITLE:** Experimental evidence of warming-induced disease emergence and its  
4 prediction by a trait-based mechanistic model

5  
6 **RUNNING HEAD:** Warming-induced disease emergence

7  
8 **AUTHORS:** Devin Kirk<sup>1,2,3\*</sup>, Pepijn Luijckx<sup>4\*</sup>, Natalie Jones<sup>5</sup>, Leila Krichel<sup>1</sup>, Clara  
9 Pencer<sup>1</sup>, Péter Molnár<sup>1,6</sup>, Martin Krkošek<sup>1</sup>

10  
11 \* Represents equal author contributions

12  
13 **AFFILIATIONS:**

- 14 1. Department of Ecology and Evolutionary Biology, University of Toronto,  
15 Toronto, Canada.  
16 2. Current address: Department of Biology, Stanford University, Stanford, USA.  
17 3. Current address: Department of Zoology, University of British Columbia,  
18 Vancouver, Canada.  
19 4. School of Natural Sciences, Zoology Department, Trinity College Dublin,  
20 University of Dublin, Dublin, Ireland.  
21 5. School of Biological Sciences, University of Queensland, Brisbane, Australia  
22 6. Laboratory of Quantitative Global Change Ecology, Department of Biological  
23 Sciences, University of Toronto Scarborough, Toronto, Canada.  
24

25 **CORRESPONDING AUTHOR:** ° kirkd@stanford.edu

26  
27 **KEYWORDS:** temperature, thermal ecology, parasite, MTE, Daphnia magna, Ordospora  
28 colligata  
29  
30

31 **Model parameterization and assumptions**

32 The population-level model is listed in the main text in Eq. 1-4, with the expression for  
33  $R_0$  listed in Eq. 5 and the thirteen parameters listed in Table 2. Seven parameters were  
34 modeled as temperature independent. The input rate of susceptibles ( $\phi_S$ ) and infecteds ( $\phi_I$ )  
35 was determined by experimental conditions and the prevalence of infections in the stocks  
36 from which exposed individuals were introduced into the experiment ( $\phi_S = 3.535 \text{ d}^{-1}$   $\phi_I =$   
37  $0.465 \text{ d}^{-1}$ ). Twelve of the ~170 individuals were harvested every three days; therefore,  
38 harvesting rate ( $h$ ) was set to  $0.0235 \text{ d}^{-1}$ . Environmental spore mortality was set to equal

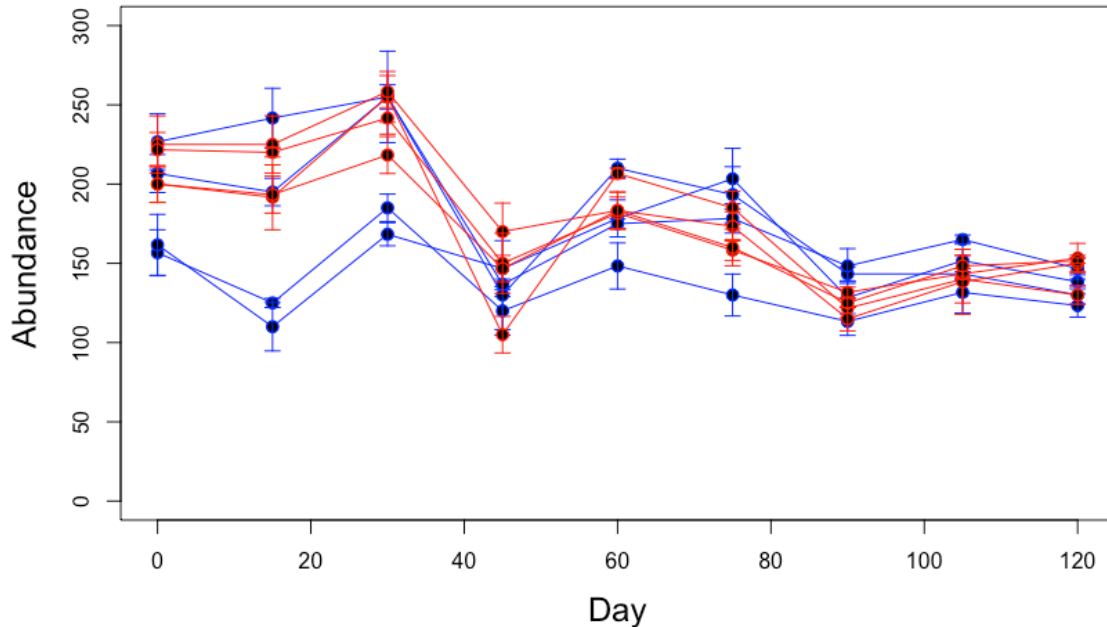
39 the rate at which we removed medium (3 of the 35L / 3 days):  $\gamma = 0.0286 \text{ d}^{-1}$ . Infected  
40 corpse degradation rate ( $\theta$ ), which does not affect  $R_0$  but affects the timing of how  
41 quickly spores are released into the environment, was set to  $0.1 \text{ d}^{-1}$ . This is the average  
42 degradation rate in an independent experiment that we conducted, where we visually  
43 assessed the time point at which the *Daphnia* gut was completely degraded (mean  
44 degradation rate =  $0.108 \text{ d}^{-1}$ , standard deviation =  $0.0659$ ; Kirk et al. unpublished data).  
45 We note that this value ( $0.108 \text{ d}^{-1}$ ) was averaged across nine experimental temperatures  
46 ( $5^\circ\text{C} - 32^\circ\text{C}$ ) and that the experiment used *Daphnia* of varying sizes, and while  
47 degradation did increase with temperature, we did not use MTE to model it, as the  
48 parameter does not appear in the  $R_0$  equation (Eq. 5) and therefore does not affect the  
49 critical transition temperature to an epidemic. Maximum recruitment rate ( $\psi$ ) was set to  
50  $1.33 \text{ d}^{-1}$  to allow for population abundances to remain around the carrying capacity  $K$ ,  
51 which was set to 170 to mirror the approximate abundances in the experiment (Fig. S1).  
52 Finally, since we did not measure *Daphnia* length (which can be used to infer *Daphnia*  
53 size and mass) in the experimental populations, we assumed a length of 2.7mm for the  
54 large individuals that were sampled based on previous observations of our stock  
55 populations. We explored the effects of this assumption using further simulations and did  
56 not observe any large changes in model predictions (Fig. S2).

57 To capture parameters that scaled with temperature we used five different  
58 parameterizations of MTE functions. Contact rate ( $\chi$ ) was modeled using a Sharpe-  
59 Schoolfield function (Schoolfield et al. 1981) with only an upper temperature threshold  
60 (Kirk et al. 2019, Fig. 1), and standardized to the volume of the container (35L) with  
61 *Daphnia* size set to  $2700\mu\text{m}$ . The probability of infection after contact ( $\sigma$ ) arises from a

62 Sharpe-Schoolfield model with upper and lower temperature thresholds that predicts the  
63 infection rate within the host, as well as how long the parasite remains in contact with the  
64 host (residence time of the parasite in the gut), which in turn is determined by *Daphnia*  
65 filtration rate (i.e.  $\chi$ ), algae concentration, and the size of the *Daphnia* (Kirk et al. 2019,  
66 Fig. 1). Previously, we modeled natural mortality using a two-parameter Weibull  
67 distribution in which the hazard can change through time depending on the shape  
68 parameter (Kirk et al. 2018). Since we did not track individuals through time in this  
69 model, we here used a constant hazard rate ( $\mu$ ). To obtain this value for each temperature,  
70 we simulated our MTE Weibull model, using Sharpe-Schoolfield functions for both  
71 parameters, to predict the natural survival curve for an uninfected individual at each  
72 temperature. From this curve, we found the time point at which survival probability is 0.5  
73 (i.e. the median survival) and used this as the expected lifespan. Finally, we set natural  
74 mortality rate ( $\mu$ ) in our model to be 1 / predicted lifespan.

75 We also used the Sharpe-Schoolfield function to model equilibrium parasite  
76 abundance within the host, which rises quickly from zero to ~160 parasite clusters near  
77 10°C, and then slowly decreases as temperature increases before approaching zero  
78 clusters near 30°C (Kirk et al. 2018, Fig. 1). Since equilibrium abundance of the parasite  
79 can take months to approach in the 10 - 13.5°C temperature range (Kirk et al. 2018), we  
80 modeled infection load in our experiment as a proportion of the equilibrium abundance.  
81 We used observed infection loads from our experiment to find the average proportion of  
82 equilibrium abundance in this temperature range: 0.182. This infection load temperature  
83 function was then used to predict the parasite-induced mortality rate ( $\alpha$ ), parasite  
84 shedding rate ( $\lambda$ ) and the number of spores in the host when it dies ( $\omega$ ) for each

85 temperature. Parasite-induced mortality rate ( $\alpha$ ) was set to the product of infection load  
86 and  $5.12 \times 10^{-6}$ , the per-parasite added mortality previously estimated (Kirk et al. 2018).  
87 We note that because we did not track individuals through time, per-parasite added  
88 mortality is constant for an infected individual and cannot change through time, though it  
89 can change with the shape parameter in Kirk et al. (2018). For  $\lambda$  and  $\omega$ , which both relate  
90 to parasite spores rather than parasite clusters, we assume that a spore cluster has twenty-  
91 four spores, which is generally the average that we observe in the lab (between 16 and 32  
92 spores per clusters). For  $\lambda$ , we assumed that when a parasite cluster bursts, half of the  
93 twenty-four spores are released into the environment while the other twelve remain in the  
94 host (to either re-infect or die), and that this bursting process occurs every seven days.  
95 We note that Refardt and Ebert (2006) estimate that the parasite may burst approximately  
96 every three days at room temperature, but we assume here that this takes significantly  
97 longer in our  $10 - 13.5^\circ\text{C}$  range since within-host parasite growth rate is depressed (Kirk  
98 et al. 2018). We refer readers to the main text for implications of modeling these rates as  
99 functions of temperature.



100

101 Fig. S1. *Daphnia magna* abundances in experimental populations. Blue and red points and lines represent  
 102 populations in constant 10.0°C and warming conditions respectively. Points represent the mean of three  
 103 counts for each population, and error bars represent the maximum and minimum value from these three  
 104 counts.

105

### 106 **Model sensitivity to assumptions**

107 We explored how sensitive our model results are to five different assumptions: 1)

108 infection load proportion of equilibrium abundance, 2) *Daphnia* size, 3) spores per

109 cluster, 4) cluster burst time, and 5) the number of spores released out of the host per

110 cluster. Assumptions were tested by simulating our model 250 times (without

111 demographic stochasticity) in which we allowed parameters to take a value from along

112 uniform distributions (with replacement) in which the median is the value used for the

113 main analysis, and upper and lower range limits are our best estimates at realistic ranges

114 for the parameter values (see Table S1). While changing the assumptions incorporated

115 more variation, our results were generally robust across the entire parameter space (Fig.

116 S2).

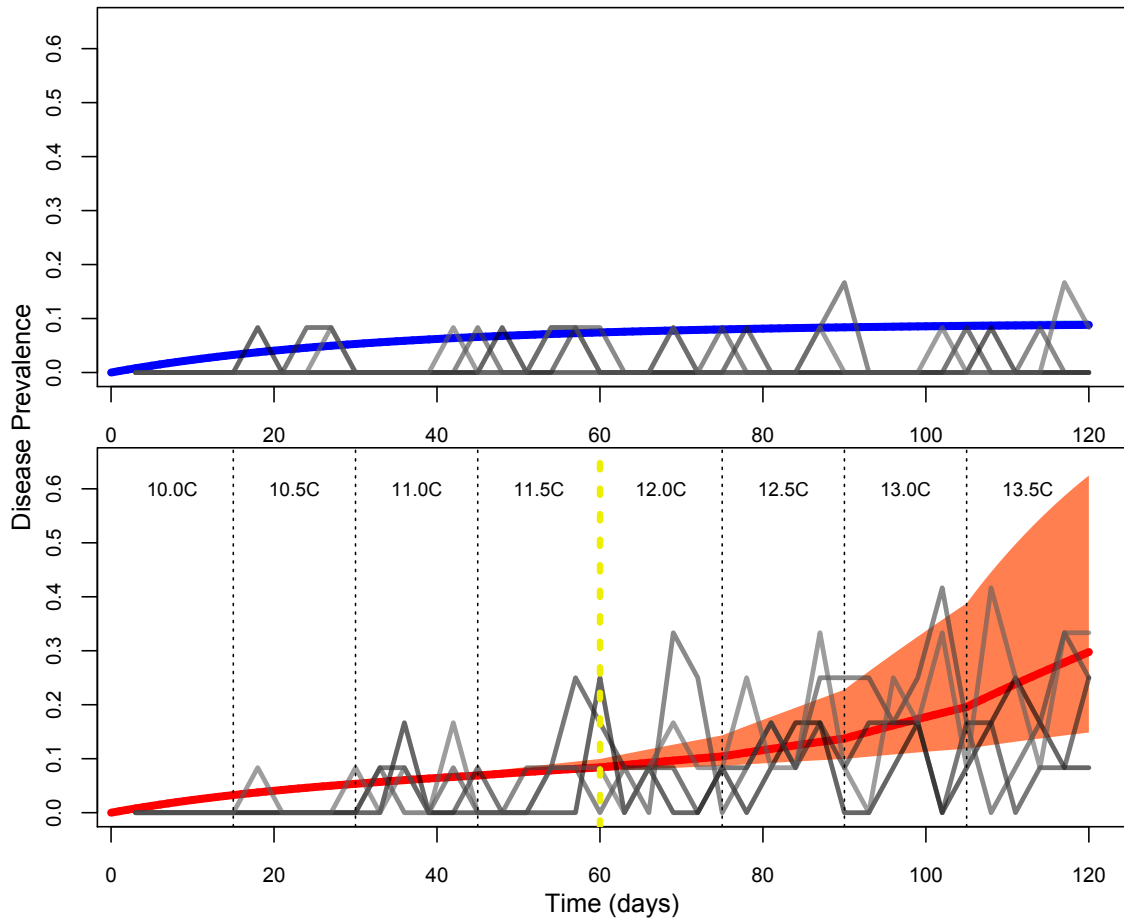
117 We also investigated the effects of sampling noise on our results, as we sampled a  
 118 subset of the population (twelve individuals) on each sampling day. We simulated the  
 119 model in a deterministic framework 250 times, and then used a binominal sampling  
 120 process to randomly select twelve individuals every three days. This process captures the  
 121 sampling noise observed in the warming samples well, but somewhat overestimates the  
 122 sampled prevalence in the constant 10°C populations (Fig. S3).

123  
 124  
 125

**Table S1. Range of parameter values used in simulations to test model sensitivity to assumptions.**

	Lower range limit	Main text value	Upper range limit
Parasite load as proportion of equilibrium parasite abundance	0.132	0.182	0.232
Parasite cluster burst time	4.5 d <sup>-1</sup>	7 d <sup>-1</sup>	9.5 d <sup>-1</sup>
Spores per cluster	16	24	32
Proportion of spores released into environment per cluster	0.25	0.50	0.75
<i>Daphnia</i> length	2500 μm	2700 μm	2900 μm

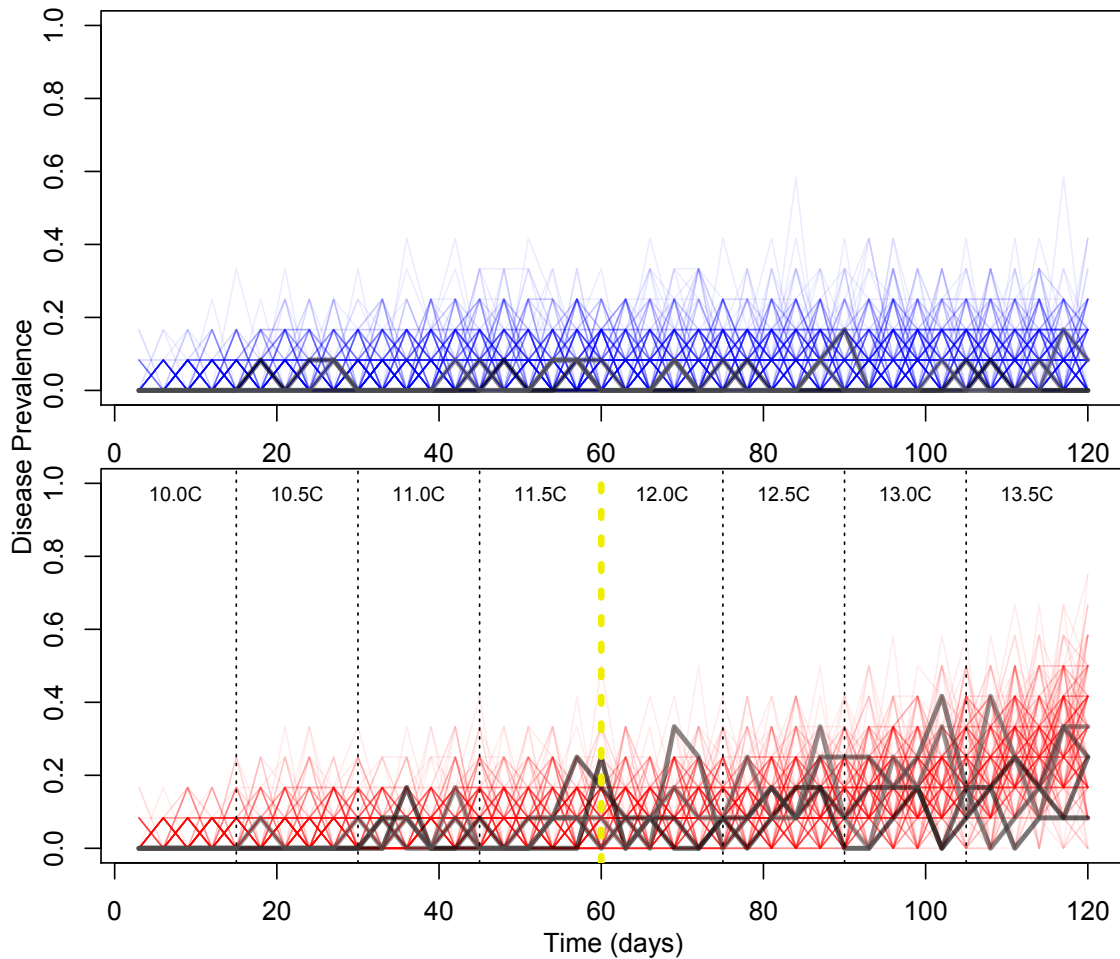
126  
 127



128

129

130 Fig. S2. Sensitivity to model assumptions. Blue (top panel) and red lines (bottom panel) represent mean  
 131 disease prevalence for constant 10.0°C and warming conditions, respectively, across 250 simulations that  
 132 sample from the parameter space. The shaded red region in the bottom panel represents the 95% confidence  
 133 interval under warming conditions. The small shaded blue region in the top panel represents the 95%  
 134 confidence interval, but is not visible due to the parameter assumptions having negligible effects on disease  
 135 prevalence at 10°C. The yellow, dashed vertical line represents the temperature/time point at which the  
 136 MTE model predicts  $R_0 > 1$  for warming conditions.  
 137



138

139 Figure S3. Effects of sampling noise. Blue and red lines represent 250 random samples from deterministic  
 140 simulation of the model. Grey lines represent experimental data for constant 10.0°C (top panel) and  
 141 warming populations (bottom panel) respectively.

142

143

144

145

146 **Observed versus predicted prevalence**

147

148 The goal of this work was not to specifically quantify model performance, but rather to

149 leverage an experimental system to provide a proof of principle that the MTE approach

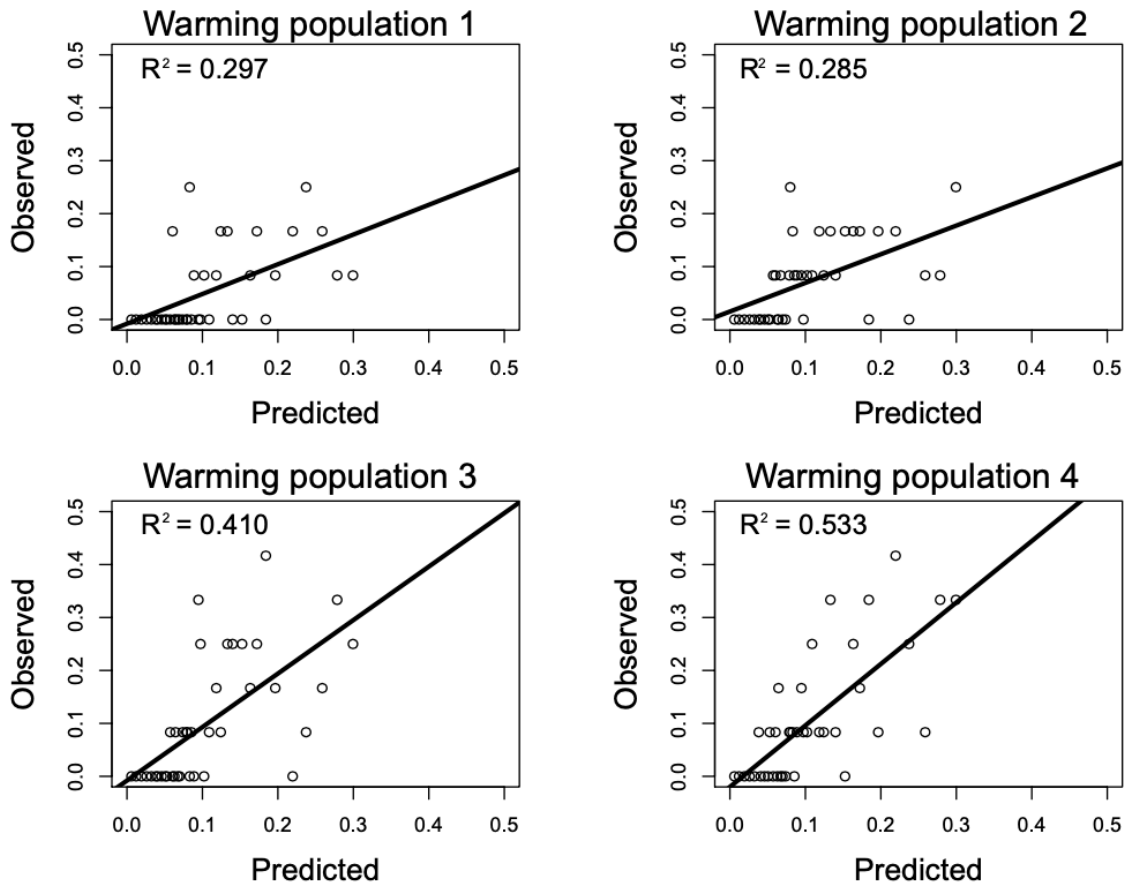
150 can be used to predict warming-induced disease emergence. Nevertheless, below we

151 provide observed versus model predicted values of disease prevalence for our four

152 warming populations. We note that observed prevalence values are discretized at only six



153 different levels due to sampling (i.e. 0/12 infected, 1/12 infected... up to 5/12 infected),  
154 while the model predicts prevalence continuously as it is averaged across our 250  
155 stochastic simulations.  $R^2$  values ranged from 0.297 – 0.533 across the four warming  
156 populations.



157  
158 Figure S4. Experimentally observed versus model predicted values of prevalence for the four warming  
159 populations.  $R^2$  values are provided for each population.  
160

161  
162  
163  
164  
165

166 **R<sub>0</sub> formulation**

167 In our R<sub>0</sub> formulation (equation 5 of the main text, reproduced as Eq. S1 here), the  
168 first term in parentheses represents the total number of spores produced per infected  
169 individual, on average.

$$R_0(T) = \left( \frac{\lambda(T)}{\mu(T) + \alpha(T) + h} + \omega(T) * \frac{(\mu(T) + \alpha(T))}{(\mu(T) + \alpha(T) + h)} \right) \left( \frac{\chi(T) * \sigma(T) * S_{eq}}{\gamma} \right) \quad \text{Eq. S1}$$

170

171 In this first term,  $\frac{\lambda(T)}{\mu(T)+\alpha(T)+h}$  represents the number of spores shed by an infected  
172 individual during their lifetime, and  $\omega(T) * \frac{(\mu(T)+\alpha(T))}{(\mu(T)+\alpha(T)+h)}$  represents the number of spores  
173 released by an infected individual after they die, weighted by the fraction of infected  
174 hosts that remain in the system until death and are not harvested prior.

175 The second term in parentheses represents the probability a spore infects a new host  
176 as opposed to being lost via medium removal, and has two key assumptions:

- 177 1) Spores that are ingested but do not infect the host are expelled, re-enter the water  
178 column, and remain viable;
- 179 2) The rate of spore loss from the water column due to ingestion and subsequent  
180 infection is very small compared to spore loss via media removal; i.e.,  $\sigma\chi S \ll \gamma$ .

181 Regarding assumption 1, to our knowledge, there have been no studies in this host –  
182 parasite system that investigate the proportion of spores that remain viable after passing  
183 through the host gut. However, evidence from a similar system with this same host and a  
184 bacterial parasite, *Daphnia magna* – *Pasteuria ramosa*, shows that the parasite is not  
185 killed if it fails to infect the host (King et al. 2013). Moreover, based on our observations  
186 working with this system, we believe that at least a large proportion of spores must

187 remain viable after passing through the host gut. This is because an average sized  
 188 *Daphnia* filters ~1ml of medium per hour (Kirk et al. 2019), meaning that the dense  
 189 populations we maintain under lab conditions (~200 hosts/2L at 20C) should filter  
 190 through all of their medium in their mesocosm every 10 hours. If spores not causing  
 191 infection were destroyed upon ingestion, this scenario would lead to very low levels of  
 192 spores in the medium resulting in little or no infection in the population, which is not  
 193 concordant with the high levels of infection prevalence we regularly observe in our stock  
 194 populations (47% prevalence, ref: this study). Moreover, we know that new viable spores  
 195 are released after host cell lysis within the anterior of the *Daphnia* gut. These spores then  
 196 must pass through the remainder of the gut before entering the environment, implying  
 197 that passage through the gut does not kill spores. Finally, microsporidian spores are  
 198 generally durable, and have been shown to survive months of winter in other *Daphnia* –  
 199 microsporidian systems (Ebert 2005).

200 With the assumption that ingested spores that do not cause infection remain viable  
 201 after passing through the gut, the probability that a spore causes an infection is

$$202 \quad [\sigma\chi S / (\chi S + \gamma)] * \sum_{i=0}^{\infty} [(1 - \sigma)\chi S / (\chi S + \gamma)]^i \quad \text{Eq. S2}$$

203 where  $\chi$  is the filtrate rate,  $\sigma$  is the probability that an ingested spore causes infection,  $S$  is  
 204 the abundance of susceptible hosts, and  $\gamma$  is the rate of medium exchange. This equation  
 205 represents the sum of the probabilities that a spore infects a host upon its first ingestion  
 206 ( $i = 1$ ), or that it passes through the gut on its first ingestion and infects a host the  
 207 second time it is ingested ( $i = 2$ ), or that it passes through the host gut for the first two  
 208 ingestions and infects a host on its third ingestion ( $i = 3$ ), and so on. Via the formula for  
 209 the sum for a geometric power series the equation becomes

210

211 
$$[\sigma\chi S/(\chi S + \gamma)] * [1 - (1 - \sigma)\chi S/(\chi S + \gamma)]^{-1} \quad \text{Eq. S3}$$

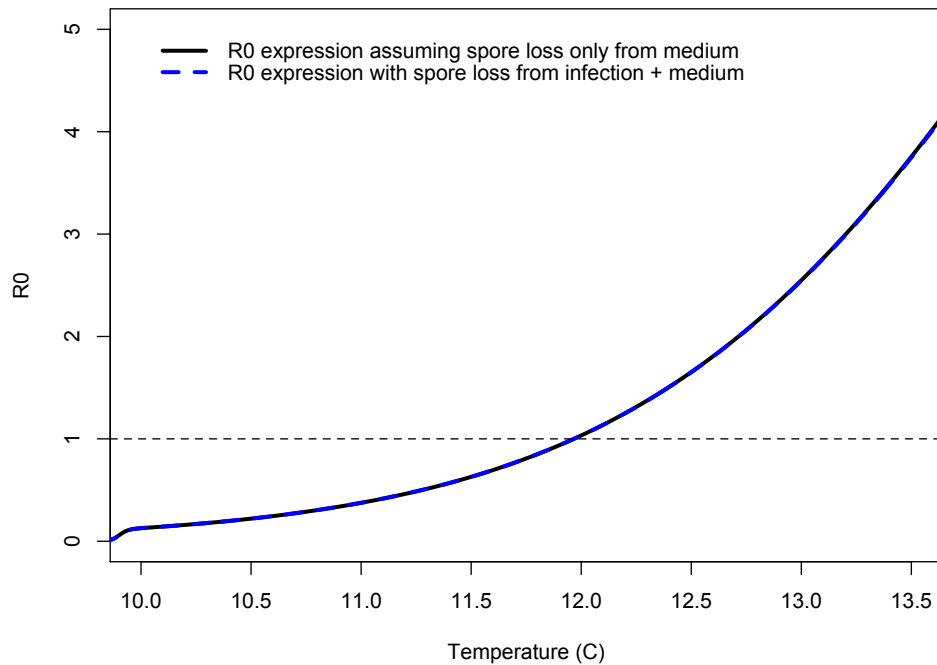
212 which simplifies to

213 
$$\sigma\chi S/(\sigma\chi S + \gamma) \quad \text{Eq. S4}$$

214 We therefore assume there are only two ultimate fates for a spore: either it is ingested  
215 and infects (at rate  $\sigma\chi S$ ) or it is removed from the system via medium exchange (at rate  
216  $\gamma$ ). Additionally, spores could of course also die in the environment, but microsporidian  
217 spores are highly durable and we assume their death rate is negligible over the timescale  
218 of the experiment as we have noted in the main text.

219 Under the approximation that  $\sigma\chi S \ll \gamma$ , we arrive at the expression for the second  
220 parenthesis for  $R_0$ :  $\sigma\chi S/\gamma$ , but as an approximation rather than exactly correct.

221 This assumption that  $\sigma\chi S \ll \gamma$  is strongly supported for our system, as we know that  $\sigma$  is  
222 very small (Kirk et al. 2019). For example, at 12°C,  $\sigma\chi S=0.000018 \text{ d}^{-1}$ , while  $\gamma$  is  
223 constant across temperature and equals  $0.0286 \text{ d}^{-1}$ . This means that spore loss from  
224 medium exchange ( $\gamma$ ) is nearly 1600x larger than spore loss from infection ( $\sigma\chi S$ ) at this  
225 temperature, and the assumption that  $\sigma\chi S \ll \gamma$  is valid. Because of this, if we look at the  
226 temperature range of the experiment (10°C -13.5°C), there is no discernible difference  
227 between predictions from the simpler  $R_0$  expression (Eq. 5) that assumes spore loss only  
228 from medium removal (black line; Fig. S2) compared to a more complicated expression  
229 that explicitly accounts for removal of spores from infection (dashed blue line; Fig. S5).



230

231 Fig. S5. Comparing  $R_0$  expressions in relation to temperature, with (black line) and without  
 232 (dashed blue line) the assumption that spore loss from infection is negligible compared to spore  
 233 loss from medium removal. The temperature range of our experiment was 10.0°C – 13.5,

234

235

## REFERENCES

- 236 King KC, Auld SKJR, Wilson PJ, James J, Little TJ. 2013. The bacterial parasite  
 237 *Pasteuria ramosa* is not killed if it fails to infect: implications for coevolution.  
 238 *Ecol. Evol.* 3:197-203.
- 239 Kirk D., Jones N., Peacock S., Phillips J., Molnár P.K., Krkosek M., et al. 2018.  
 240 Empirical evidence that metabolic theory describes the temperature dependency  
 241 of within-host parasite dynamics. *PLOS Biology* 16:e2004608.
- 242 Kirk, D., Luijckx, P., Stanic, A., Krkosek, M. 2019. Predicting the thermal and allometric  
 243 dependencies of disease transmission via the metabolic theory of ecology. *The*  
 244 *American Naturalist*. 193: 661-676.
- 245 Refardt, D., Ebert, D. 2006. Quantitative PCR to detect, discriminate and quantify  
 246 intracellular parasites in their host: an example from three microsporidians in  
 247 *Daphnia*. *Parasitology* 133:11-18.
- 248 Schoolfield, R.M., Sharpe, P.J.H., & Magnuson, C. E. 1981. Non-linear regression of  
 249 biological temperature-dependent rate models based on absolute reaction-rate  
 250 theory. *Journal of Theoretical Biology* 88:719–731.